J. Condensed Matter Nucl. Sci. 19 (2016) 287–297

Research Article

Impact of Electrical Avalanche through a ZrO_2–NiD Nanostructured CF/LANR Component on its Incremental Excess Power Gain

Mitchell R. Swartz* and Gayle Verner

Nanortech Inc., Wellesley Hills, MA 02481-0001, USA

Peter L. Hagelstein

Research Laboratory of Electronics, Massachusetts Institute of Technology, Cambridge, MA 02139, USA

Abstract

Cold fusion nanomaterials, in general, and NANOR®-type LANR components (derived from them), in particular, have two distinct regions of performance on each side of the electrical avalanche. This had lead to the identification of three (3) distinct regions of their electrical operation. We now report that the optimal power gain of NANOR®-type cold fusion components is found far below the breakdown voltage and that the power gain decreases continuously as the electrical avalanche threshold is approached. Beyond the region of electrical avalanche, the previously active preloaded LANR quantum electronic components then give a thermal output similar to a standard ohmic control (a carbon composition resistor). Therefore, use of this technique of driving an active CF/LANR nanomaterial component into, and beyond, their avalanche threshold, provides verification of the excess heat an additional way, which confirms that the calorimetry was calibrated. Also, this investigation indicates where, on the input power axis, to drive them for a maximum effective use. We also report that deuterium can fuel nanomaterial ZrO_2–Ni systems, consistent with the previously report involving aqueous CF/LANR systems by Swartz et al. (ICCF-9).
 ISSN 2227-3123

Keywords: Deuterated nickel, Nanomaterials, Nanostructured ZrO_2, ZrO_2–NiD

1. Introduction

Active cold fusion dry nanomaterials, both unloaded and preloaded with D or H, have three regions of electrical operation, as discussed below in detail. We report the continuous measurement (and loss) of excess heat production from an active CF/LANR component during and after its electrical breakdown, namely the, avalanche state. This transformation of active CF/LANR components from active to inactive state will be shown to be not only critical to successfully understanding and controlling these energy producing reactions, but also, providing a significant and giant step forward.

*Corresponding author. E-mail: mica@theworld.com

 ISSN 2227-3123

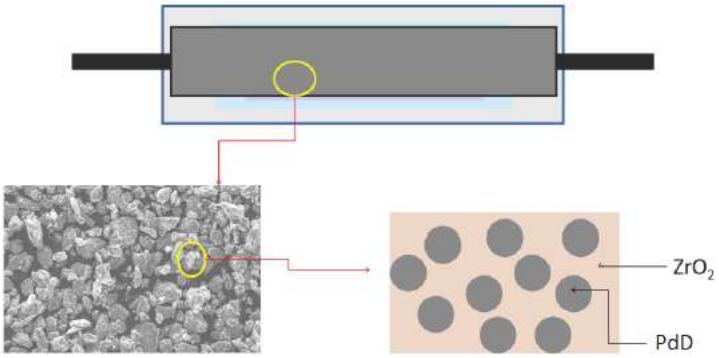

Figure 1. A schematic and actual view of an early NANOR®-type component. (*Top*) Shown is the two terminal component with the cylindrical shaped core. (*Bottom left*) A scanning micrograph shows the nanomaterial in the core. (*Bottom right*) A schematic illustration of the electrically insulating zirconia within which lie islands of deuterated alloy.

2. Background. A new generation of CF components

Dry ZrO_2–PdNiD NANOR®-type cold fusion or lattice assisted nuclear reaction (CF/LANR) components containing activated nanocomposite ZrO_2–PdNiD and ZrO_2–PdD which are preloaded with deuterons (thereby avoiding requisite loading each time) are capable of producing excess heat with significant energy gain [1,2] over long periods of time with reasonable reproducibility and control. These self-contained, two-terminal nanocomposite ZrO_2–PdNiD CF/LANR components feature new composition, structure, and superior handling properties (enabling portability and transportability) compared to aqueous and/or gas-loaded cold fusion (LANR) systems. They represent a new generation of LANR (CF) quantum electronic devices which are active and demonstrate significant improvement over all of their predecessors both regarding in sustained activity, improved reproducibility, and a large incremental power gain ($P_{\mathrm{output}}/P_{\mathrm{input}}$).

The initial NANOR®components are smaller than 2 cm length, and with 30–200 mg of active LANR material. For these NANOR®-type LANR components, the fuel for the nanostructured material is deuterium which is contained in the core volume (or chamber), a hermetically sealed enclosure.

The enclosure is tightly fit because both contamination is a potential problem and because of the potential toxicity, from the nanomaterial. Early NANOR®-type CF/LANR components were made of nano-scale regions of PdD, PdNiD or NiD in ZrO_2 [3,4]

Later, NANOR®-type LANR devices were loaded with additional D for greater loadings (ratio of D to Pd) which are estimated at 100–130% or more, although additional shallow traps are not ruled out. Thus, the deuterons are tightly packed ("highly loaded") within the nanostructured lattices [4]. Although the correct terminology is ZrO_2–$PdNiD_{1.3}$, for simplicity this subscript is left off.

Lattice assisted nuclear reactions (LANR or cold fusion) use such highly loaded hydrogen alloys to create heat and other products [5]. They do this by enabling deuterium fusion to form an excited *de novo* helium nucleus (^{4}He*) at near room temperature, under difficult-to-achieve conditions. The product is believed to be *de novo* ^{4}He based on previous CF/LANR studies in aqueous systems, such as by Miles [5]. The "excess heat" observed is energy derived from the subsequent coherent de-excitation of the ^{4}He* to its ground state via an internal conversion using the lattice

phonons. Here, the excess heat is stimulated by the applied electric current; and the deuterium loading is separated from the excess heat operation.

Usually, in the past, successful LANR required engineering of multiple factors including loading, adequate confinement time, loading rate, and prehistory (with careful avoidance of contamination and materials and operational protocols which quench performance). Today, dry, preloaded NANOR®-type technology makes LANR reactions more accessible. What is different here is that most importantly, the components are pre-loaded so that LANR activation of the desired cold fusion reactions is, for the first time, separated from loading. In every other system known, Fleischmann and Pons, Arata, Miles, and the others, the loading has been tied to activation at room temperature [6].

2.1. States of CF/LANR electrical drive

It is a long, expensive, arduous effort to prepare these preloaded nanocomposite CF/LANR components, but by contrast, in these pre-loaded NANOR®-type CF/LANR components, the desired reactions are driven, and activated, by an applied electrical current. The development of more reproducible nanostructured CF/LANR components has not been easy, and has directly been linked to improved materials, with complete avoidance of low-threshold electrical breakdown states with their electrical avalanches and their CF/LANR quenching tendencies [1,2,4].

However, until now we have never completely measured the heat production from the active component on both sides the electrical breakdown (avalanche) state. This is important because although we have reported both the observed excess heat on one side of the electrical avalanche and the quenching of that excess heat on the other side, until now we have never observed both with continuity (observable in Fig. 1). This transformation of active CF/LANR components from active to inactive states has been critical to successfully controlling CF/LANR, and is critical to understanding how to engineer these systems.

2.2. Preliminary early results, including five month open demonstration at MIT

Early NANOR®-type components have been deliberately engineered to be small and low power (Excess power gain, P_{xs}, of hundreds of milliwatts) to enable them to be carefully evaluated for energy gain, including during, and after, the January, 2012 IAP MIT Course on CF/LANR. This public demonstration ran from Jan. 30, 2012 through mid-May 2012 [2]. A Series 6 NANOR®-type CF/LANR component provided long term CF/LANR activity and was monitored by parallel diagnostics including calorimetry, input-power-normalized delta-*T*, and focused heat flow measurement (such as Omega HFS Thin Film) and calibration with an ohmic (thermal) control located next to the NANOR®. The NANOR and the thermal control were at the center of much larger thermal mass in the calorimeter discussed in more detail in [1,2].

The NANOR®-type preloaded LANR device openly demonstrated clear cut energy gain. Over weeks, the NANOR®-type preloaded LANR component openly demonstrated energy gain (COP) which ranged generally from 5 to 16 (e.g. 14.1 (~1412%) while the MIT IAP course was ongoing, [11]) confirmed by three methods and time integration. It was driven for more than a year with careful evaluation for energy gain under a variety of conditions. The excess energy gain compared to driving input energy exceeded 20 times (sometimes more). This NANOR®-type preloaded LANR system had a much higher energy gain compared to the 2003 CF/LANR demonstration unit using an aqueous high impedance system with a Phusor®-type electrode (energy gain 14.1 in 2012 vs an energy gain ~2.7 in 2003). It also had an improved controlling/driving system which provided a reliable low power, high-efficiency, energy production component for demonstration and teaching purposes of size smaller than a centimeter, with an active site weight of less than 50 mg. Although small in size, this NANOR®-type preloaded LANR device is actually not *de minimus* because the LANR excess power density is more than 19,500 W/kg of nanostructured material [1] and the carbon footprint is zero.

3. Experimental

3.1. Materials - Impact of E-field on nanomaterial

Nanostructured materials are important in LANR and are also produced in codeposition structures, observed producing non-thermal near infrared emissions when active, and exhibit typical CF/LANR excess heat correlated with the size of the Pd–D nanostructures [4,5]. However, the development of more reproducible nanostructured CF/LANR components has not been easy, and has directly been linked to improved materials, with complete avoidance of low-threshold electrical breakdown states with their CF/LANR quenching tendencies. The problem is that there exist three operating regions and one involves electrical breakdown (electrical avalanche transconduction).

Avalanche behavior with three regions were first observed with ZrO_2–NiH NANOR®-type component [4]. Control of these breakdown states and quenching tendencies has been critical and has also required surmounting the extremely high electrical resistances (as high as hundreds of gigohms) of these nanomaterials [1,3] and their complicated polarization/transconduction phenomena including an electrical current "avalanche (transconduction electrical breakdown) effect" which has a critical negative role on excess heat generation because it quenches the desired reactions even as the input power increases. The very high DC electrical impedances can suddenly drop, as the voltage across the sample (transsample voltage) is increased to as low as ~ 24 V. It can be shown theoretically that this sudden reduction can be attributed to an "avalanche effect" that is typical of the current–voltage behavior that occurs in Zener diode, but perhaps better understood as follows.

The nanostructured material is a composite distribution of nanostructured ferromagnetic "islands" separated among a vast dielectric zirconia "ocean". The dielectric zirconia embeds uncountable numbers of nanostructured metal ternary alloy islands. The high resistance occurs because the zirconia dielectric matrix is insulating at low voltage and it keeps the nanoscale metal islands electrically separated and prevents the aggregation of the islands. Each nanostructured island acts as a short circuit elements during electrical discharge. One hypothesis of the excess heat is that these "islands" allow deuterons to form a hyperdense state in each island, where the deuterons thereafter are able to be sufficiently close together to fuse and form ^{4}He*, by some pathway not known involving paired deuterons or possibly more.

There have been important implications from the fact that NANOR®-type component current and voltage characteristic shows a breakdown effect. For example, some electronics destroyed when voltage exceeded NANOR®-type component breakdown voltage [7]. Therefore, an effort was made to develop more robust electronics capable of driving the NANOR®-type component through breakdown and on both sides

3.2. Methods - Electrical activation of NANOR®-type CF/LANR component

The LANR preloaded, stabilized NANORs were driven by a high DC voltage circuit up to 1000+ V rail voltage. The duty cycle was split into a rest period with no input to anything, followed by a period with input power going to a control portion, and then to the CF/LANR component. That was followed by another rest period and control portion. The input power was delivered by a carefully controlled electrical DC pulse. The control was an ohmic resistor which was used to thermally calibrate the calorimeter by providing a series of well known input power, and by using a precise amount of time, energy-measured pulses [1,2]. Data acquisition was taken from voltage, current, temperatures at multiple sites of the core, around the heat flow sensor, and outside of the calorimeter. Data acquisition sampling was at data rates of 0.20–1 Hz, with 24+ bit resolution; voltage accuracy $0.015^{+/-0.005}$ V, temperature accuracy < 0.6°C). The noise floor (power) of the calorimeter is in the range of ∼1–30 mW. The noise power of the Keithley current sources is generally ∼10 nW. The implication of this is that the excess power generated (if it is present) must exceed the noise floor of the calorimeter in order to be observable. It also means that the driving of the calorimeter below that noise floor can on occasion result in false positives without further techniques to rule this out [8].

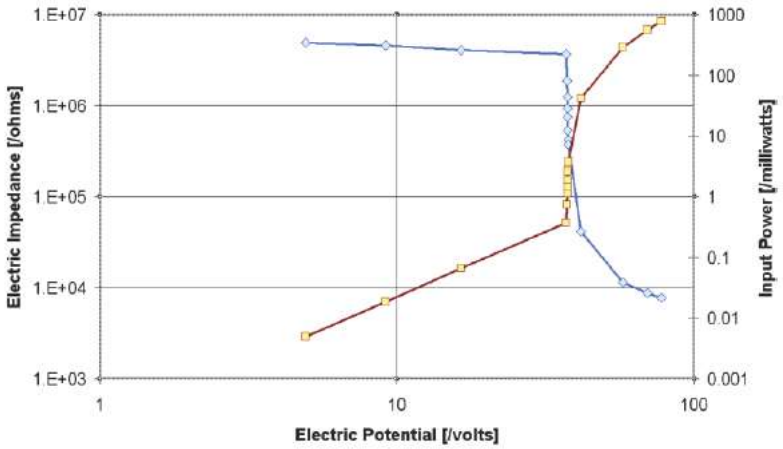

Figure 2. Impedance and Electrical current as a function of applied electric potential (volts). This figure shows the response, and particularly the Avalanche behavior with three regions, as first observed with ZrO_2–NiH NANOR®-type component. Three regions are seen; consisting of the initial plateau of electrical impedance, then the rapid fall off, and finally a sloped region at higher voltage [4,1].

Input power is defined as $V \times I$. There is no thermoneutral correction in denominator. Therefore, the observed incremental power gain is actually a lower limit. The result is heat measurement of this preloaded NANOR®-type LANR three (3) ways ending in calorimetry, input-power-normalized delta-T ($\mathrm{d}T/P_{\mathrm{in}}$), and input power normalized heat ($\mathrm{HF}/P_{\mathrm{in}}$) [11]. These three methods of verification are pooled to derive very useful information, including the energy produced ("excess energy") and sample activity. The instantaneous power gain (power amplification factor (non-dimensional)) is defined as $P_{\mathrm{out}}/P_{\mathrm{in}}$. As discussed above, the energy is calibrated by at least one electrical joule control (ohmic resistor) used frequently, and with time integration for additional energy validation. The excess energy, when present, is defined as (P_{output} - P_{input})$\times$ time. The amount of output energy (and therefore, both power, and energy, gain) is determined from the heat released producing a temperature rise, which is then compared to the input energy. The output of the component compared to the output of the precisely driven ohmic control.

4. Results

4.1. Interesting transconduction/XSH results and NiD can yields XSH

The new results are interesting. First, we continue to see improvements in loading and fabrication with each new generation of NANOR®-type components with respect to excess power gain and excess heat (XSH) At the time this manuscript was initially submitted, the Series 7 NANOR®-type components were the best so far with respect to incremental power gain; under select conditions very high (>1000) power gains observed. These components have demonstrated the first evidence of Mode B behavior [9], where an activation energy is not required beyond the input. Second, the new NANOR data reveals (as was shown for aqueous CF/LANR systems at ICCF-9) that deuterium can fuel ZrO_2–Ni systems, too [10].

4.2. Imaging a CF/LANR component through the electrical avalanche

Third, as shown in detail below, it is now possible to take electrical and calorimetry data systematically in the different regions of the electrical avalanche, and on both sides of that avalanche. Figures 3–6 show the examination of

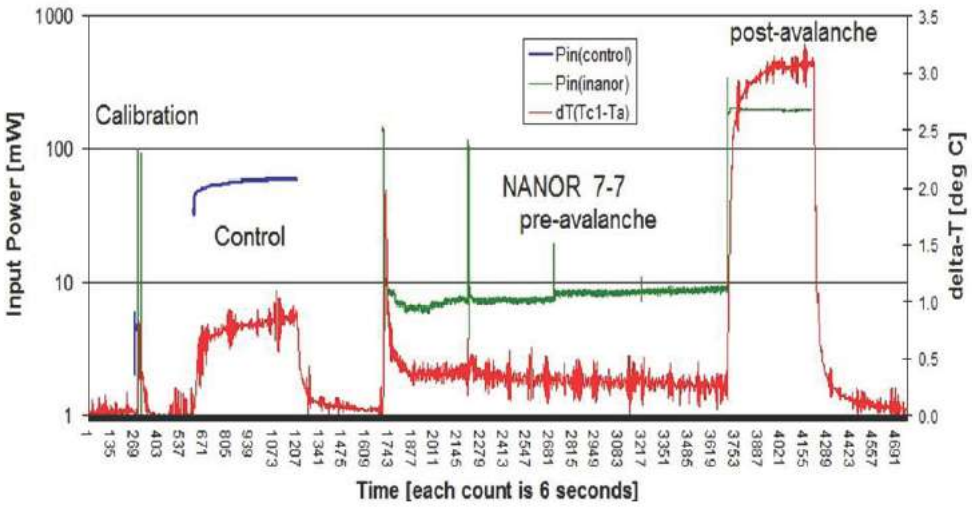

Figure 3. Temperature difference induced by a ZrO_2–NiD NANOR®-type component and ohmic control, both electrically driven, showing both excess heat and avalanche behavior.

this ZrO_2–NiD NANOR®-type component looking for possible excess heat on both sides of the electrical avalanche, and from several points of view. The figures include both raw data (Fig. 3) and derived information from the runs (Figs. 4–6). They demonstrate conclusively that LANR excess energy can be achieved, and it is heralded by input power normalized incremental temperature (delta-T) changes shown in Fig. 4, and verified and confirmed by calorimetry (Fig. 5).

Figure 3 is a set of curves which plot the differential incremental increase in temperature (°C) for the case with no input ("Background"), for the case of an ohmic thermal control (labeled 'control') at the same location, and for the NANOR®-type LANR component, both pre- and post-avalanche. The curves in Fig. 3 plot the raw data as the incremental temperature rise and the applied input electrical power. The applied electrical power is switched between an ohmic (thermal) control and the self-contained
quantum electronic Series 7 NANOR®-type component CFLANR component. The graph presents these three curves and demonstrates the temperature rise in response to several different levels of electrical input power administered to both the ohmic control and then to the NANOR. For each of those electrical input powers, shown is the input power and then induced incremental output temperature rise.

There is shown an initial calibration pulses at the very beginning of the sequence, which is used for accuracy and precision checks of voltages and currents. The x-axis represents time, and each count represents 6 s. The y-axis on the left side represents electrical input power in watts. The y-axis on the right side represents the amount of temperature rise (differential temperature increase) in response to the electrical input power (degrees Centigrade). The graph shows first the response to the calibration pulse, then the response of the ohmic control, and then the response of the NANOR. A very large rise in power input and output (delta- T) result after the electrical avalanche at about count 3700.

Compare the output for NANOR®-type LANR component to the thermal (ohmic) control in Fig. 3. Two distinct regions of performance are seen on each side of the avalanche which is labeled in Fig. 4.

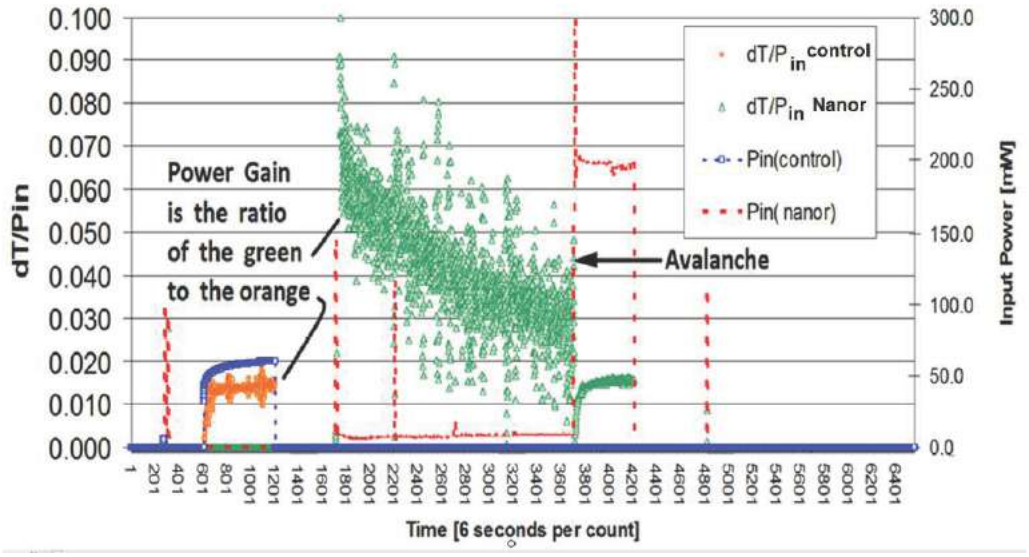

Figure 4. These curves show the dT/P_{in} ratios, which enable determination of the power gain, both in the excess heat region and after the avalanche behavior, for a ZrO_2–NiD NANOR®-type component. The region of the Avalanche is labeled.

4.3. On other side of the avalanche the power gain is essentially unity

To determine the effectiveness of the heat source, Fig. 4 is set of curves which presents the results of the same experiment, but which plots the temperature rise (delta-T in °C) of the preloaded NANOR®-type LANR component and the ohmic control with both normalized to input electrical power. This derived value, delta-T/P_{in}, is important because it enables semiquantitative determination of the incremental power gain.

Figure 4 shows the differential temperature rise normalized to input electrical power for the preloaded NANOR®-type LANR component, and for the case with no input power ("Background" but not labeled in the figure), and for the case of input to the ohmic thermal control, located at the core. The x-axis represents time, and each count represents 6 s. The y-axis on the left side represents electrical input power in watts. Each of the outputs are read off on the right-hand side. The y-axis on the right side represents the amount of temperature rise (differential temperature increase) normalized (that is, divided by) to the electrical input power. The units of this axis are in °C/W. A calibration pulse, used for accuracy and precision check of voltage and current measurement, is again also shown at the beginning and end (not labeled) of the run.

Because these curves plot the temperature rise normalized to input electrical power as a function of time, the ratios can be used to estimate incremental power gain. That is done here by taking the ratio of the response of the NANOR (green) to the ohmic control (orange). Compare the delta-T output normalized to input power for preloaded NANOR®-type LANR component to the thermal (ohmic) control, delta-T/P_{in}.

By comparing that ratio, note the active preloaded LANR quantum electronic component again clearly shows significant improvement in thermal output, here input-power-normalized compared to a standard ohmic control (a carbon composition resistor). Observe that despite lower input electrical power to the NANOR®, the temperature rise normalized to input electrical power observed in the core was higher than expected, as compared to the ohmic control. The graph therefore shows quite clearly a demonstrated active over-unity thermal output power from the NANOR®-type cold fusion (LANR) component, before the electrical avalanche.

Attention is directed to the fact that Fig. 4 clearly demonstrates a larger, significant improvement in differential thermal output (incremental increase in temperature in °C) for the preloaded NANOR®-type quantum electronic component compared to the standard ohmic control (a carbon composition resistor), before the electrical avalanche.

Figure 4 thus heralds the significant incremental power gain, and therefore excess energy achieved, by this Series 7 NANOR® type of LANR component. The ratio discussed above indicates that the input power normalized delta-measurements suggests strongly the presence of excess heat. Quantitatively, the amount of this differential temperature increase divided by the input electrical power for the preloaded NANOR®-type component compared to the control heralds great utility, and so to the degree that these components can be improved for total power out, this is a possible future efficient heat production source.

Figure 5 is a set of curves which present the results of the same experiment, but which plots the electrical power input and the thermal output power both for the two terminal NANOR®-type component Series 7 component, the ohmic control, two control pulses, and the background (no electrical input to either components). The curves present the electrical input power at several different input electrical power levels. Evaluation of the calorimetric response of both the ohmic control and the NANOR®-type component also includes presenting electrical energy input and the thermal heat (energy) output.

The figure shows the input, and the calorimetry, of preloaded NANOR along with that for the ohmic thermal control used to calibrate the system. Those calibration pulses, used for accuracy and precisions checks of voltages and currents and time, are also shown. The input to the thermal ohmic control followed by the preloaded NANOR®-type component is shown, as are the calibrated calorimetric outputs for both. The x-axis represents time, and each count represents six (6) seconds. The$y$-axis on the left side represents electrical input power in watts. The y-axis on the right side represents the amount of energy released. The units of this axis are in joules. Each of the power and energy outputs are read off of the left and the right-hand sides, respectively. The latter curves (on the right-hand side axis) represent time integration to determine total energy. They thus rule out energy storage, chemical sources of the induced heat, possible phase changes, and other sources of possible false positives.

Compare the output of the NANOR®-type LANR component to the thermal (ohmic) control. As can be seen, this semiquantitative calorimetry, itself calibrated by thermal waveform reconstruction, was consistent with excess heat being produced only during energy transfer to the active NANOR®-type LANR component. Notice that the active preloaded LANR quantum electronic component clearly shows significant improvement in thermal output compared to a standard ohmic control (a carbon composition resistor). The graph shows quite clearly demonstrated over unity thermal output power from the demonstration-power-level NANOR-type cold fusion (LANR) component, at least during the pre-avalanche period. It is clear that Fig. 5 demonstrates the excess heat from this component versus an ohmic control.

4.4. Optimum power gain found well below breakdown voltage

Figure 6 is a curve which presents the results of the same experiment, and which plots the incremental power gain of this two terminal NANOR®-type component Series 7 component and the ohmic control. There is obvious that the incremental power gain for the CF/LANR component until the avalanche, at which time (count $\sim$3700) the component has no energy gain, but has a response similar to an ohmic resistor. This saliently demonstrates that outside of the CF/LANR active state, the component acts as any other ohmic resistor, and thus confirms that the calorimetry was calibrated, and verifies the excess heat yet an additional way.

4.5. Optimum power gain found well below breakdown voltage

In this experiment, we have for the first time obtained calorimetric data while scanning the applied electrical voltage in a series of levels, through the avalanche and then continuing on the other side of the avalanche (at even high applied

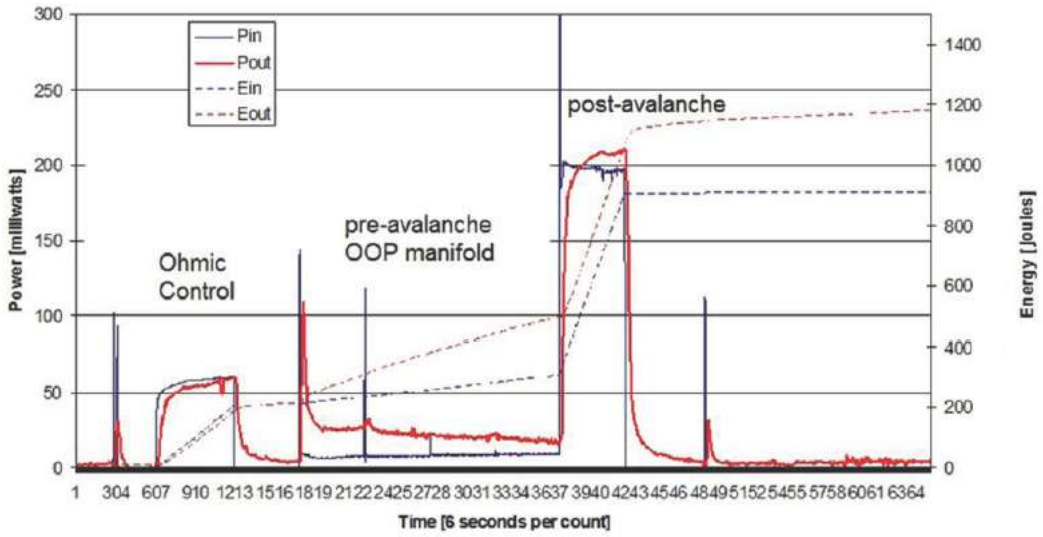

Figure 5. Four curves showing the input power and thermal power output, and their time integrals showing both excess heat and avalanche behavior, in a ZrO_2–NiD NANOR®-type component.

voltages). Thus, we have serniquantitatively measured this drop in power gain on the way to the electrical avalanche, and the total loss of that power gain during the electrical avalanche which occurs even though higher voltage is applied.

Several things have been made clear from this experimentation. First, the optimal power gain of NANOR®-type cold fusion components is found far below the breakdown voltage. This investigation has revealed that the power gain decreases continuously as the electrical avalanche threshold is approached. Second, in fact, as the voltage which produces the electrical avalanche is approached, the power gain, appears to monotonically decrease. Third, it is important to recognize the importance of our discovery of the fact that on the far side of the electrical avalanche. the power gain of the NANOR®-type component is essentially unity. Therefore, these discoveries have important imp1ications, First, it indicates where to drive these systems for at maximum effective use. Second, it indicates a key (present) limitation of these over-unity CF/LANR components.

4.6. On other side of the avalanche, the NANOR®-type component acts “dead”, providing yet an additional control

This investigation has revealed that, despite driving at higher input electrical power, on the other side of the electrical avalanche, these NANOR®-type components act as little more than electrical resistors which are conventional, not over-unity, and therefore are functionally “dead” with respect to producing excess heat. Although this appears limiting in some ways, this phenomena does provide yet an additional control to check calorimetry beyond the measurements involving simply using a simple ohmic, thermal control. Therefore, driving a component into this region thus adds an additional verification of the actual excess heat which is developed in these studies.

4.7. NiD can yield XSH

This result also demonstrates clear excess heat (XSH) can be obtained from a Ni–D nanomaterial system. This is consistent with the previously reported impact of D to the high impedance aqueous CF/LANR system [10].

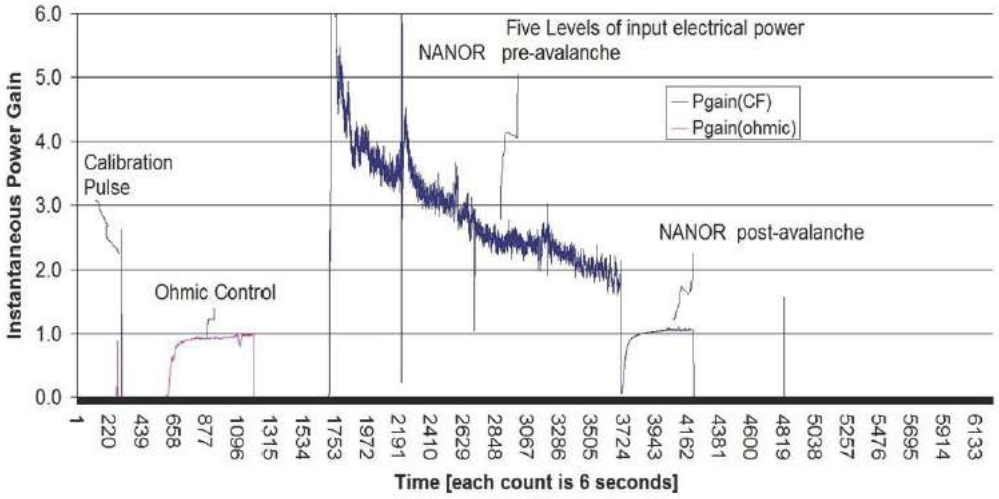

Figure 6. This graph presents the power gain of the ZrO_2–NiD NANOR®-type component CF/LANR component as a function of time, and shows that the excess heat which is generated decreases with high input power, eventually reverting to normal, ordinary, resistor-like operation after the electrical avalanche.

Swartz et al. presented at ICCF-9, the addition of D does NOT poison the reaction in the aqueous Ni system (under low drive conditions) but actually increases the incremental power gain. Only in the long run and at higher input power does D damage the Ni system [10].

5. Conclusion

5.1. Future of clean, high performance energy production components

It is clear that these preloaded nanostructured NANOR®-type CF/LANR quantum electronic components are quite useful [1,11]. They have shown significant improvement over their predecessors, including the highly successful metamaterial PHUSOR®-type of LANR component. They comprise an effective very clean, highly efficient, energy production system which has worked successfully as a test bed for cold fusion experiments for years, and has enabled the way to higher instantaneous power gain, total energy gain, imaging [12], emissions [13], open demonstrations [2,11], and a better understanding of the impact of applied magnetic fields [7], electrical transconduction [1,4], and things that quench the desired reactions (as presented at ICCF17, ICCF18, and ICCF19). Therefore these dry, preloaded, ready-to-be-activated, NANOR®-type LANR components/systems/materials, if the input power levels can be increased, may be in the future of clean efficient energy production including in preassembled IC components and systems.

Acknowledgements

The authors would like to thank Jeff Tolleson, Alex Frank, Alan Weinberg, Richard Goldbaum, Allen Swartz, Brian Ahern, Jeff Driscoll, and Charles Entenmann for their suggestions and support. This effort was supported by JET Energy Inc. and New Energy Foundation. NANOR® and PHUSOR® are registered trademarks of JET Energy

Incorporated. NANOR®-technology, and PHUSOR®-technology are protected by U.S. Patents D596724, D413659 and several other patents pending.

References

[1] M.R. Swartz, G. Verner et al., Energy gain from preloaded ZrO_2–PdNi–D nanostructured CF/LANR quantum electronic components, *J. Condensed Matter Nucl. Sci.* **13** (2014) 528. www.iscmns.org/CMNS/JCMNS-Vol13.pdf.

[2] M.R. Swartz and P.I. Hagelstein, Demonstration of energy gain from a preloaded ZrO_2–PdD nanostructured CF/LANR quantum electronic device at MIT, *J. Condensed Matter Nucl. Sci.* **13** (2014) 516. www.iscmns.org/CMNS/JCMNS-Vol13.pdf.

[3] Y. Arata and Y.C. Zhang, Observation of anomalous heat release and helium-4 production from highly deuterated palladium fine particles, *Jpn. J. Appl. Phys.* **38** (7A), Part 2 (1999) L774–L776.

[4] M.R. Swartz, LANR nanostructures and metamaterials driven at their optimal operating point, *J. Condensed Matter Nucl. Sci.* **6** (2012) 149; *LANR/LENR Sourcebook*, Vol. 3, October 21, 2011; www.iscmns.org/CMNS/JCMNS-Vol6.pdf.

[5] M. Swartz, Survey of the observed excess energy and emissions in lattice assisted nuclear reactions, *J. Scientific Exploration* **23**(4) (2009) 419–436.

[6] M. Miles et al., Correlation of excess power and helium production during D_2O and H_2O electrolysis using palladium cathodes, *J. Electroanal. Chem.* **346** (1993) 99–117.

[7] M. Swartz, G. Verner et al., Amplification and restoration of energy gain using fractionated magnetic fields on ZrO_2–PdD nanostructured components, *J. Condensed Matter Nucl. Sci.* **15** (2015) 66; www.iscmns.org/CMNS/JCMNS-Vol15.pdf.

[8] M. Swartz, Patterns of failure in cold fusion experiments, *Proc. of the 33rd Intersociety Engineering Conference on Energy Conversion*, IECEC-98-I229, Colorado Springs, CO, August 2–6, 1998.

[9] M.C.H, McKubre, F.L.Tanzella, V. Violante, What is need in LENR/FPE studies? *J. Condensed Matter Nucl. Sci.* **8** (2012) 187–197.

[10] M. Swartz, G.M. Verner, A.H. Frank, The impact of heavy water (D_2O) on nickel-light water cold fusion systems, *Proc. 9th Int. Conf. on Cold Fusion (Condensed Matter Nuclear Science)*, Beijing, China, Xing Z. Li (Ed.), May 2002, pp. 335–342.

[11] M. Swartz, G. Verner, J. Tolleson and P.L. Hagelstein, Dry, preloaded NANOR®-type CF/LANR components, *Current Science* **108** (4) (2015) 595. http://www.currentscience.ac.in/Volumes/108/04/0595.pdf.

[12] M. Swartz, G. Verner et al., Imaging of an active NANOR®-type LANR component using CR-39, *J. Condensed Matter Nucl. Sci.* **15** (2015) 81; www.iscmns.org/CMNS/JCMNS-Vol15.pdf.

[13] M. Swartz, Incremental high energy emission from a ZrO_2–PdD nanostructured quantum electronic component CF/LANR, *J. Condensed Matter Nucl. Sci.* **15** (2015) 92; www.iscmns.org/CMNS/JCMNS-Vol15.pdf.